SITE RESPONSES AND SEDIMENT STRUCTURES ALONG THE NW AND NE PROFILES IN BEIJING AREA REVEALED BY MICROTREMOR H/V SPECTRAL RATIO STUDIES

W. Wang[1], L. Liu[2,1], Q. Chen[1], and E. Rohrbach[2]

[1] *Institute of Earthquake Science , China Earthquake Administration, Beijing,100036 P. R. China*
[2] *Department of Civil & Environmental Engineering, University of Connecticut, Storrs, CT 06269, USA*
Email: wjwang@seis.ac.cn, lanbo@engr.uconn.edu

ABSTRACT :

To estimate the detailed strong ground motion caused by an earthquake for seismic hazard reduction requires high-resolution near-surface geological information. The techniques using **microtremor** measurements are cost-effective tools that rapidly acquire high-resolution sedimentary layer information over a large area about site response, sedimentary thickness, and velocity structures compared to conventional borehole drilling or active seismic exploration. In summer of 2007, we had conducted microtremor array measurements in the greater Beijing area along two roughly orthogonal profiles in the NW and NE directions centered at the Forbidden City. The profile lengths are 64 km for the NW profile and 76 km for the NE profile, respectively, with spacing interval of 200 meters for both profiles. Microtremors were recorded with the 3-component, short-period seismometers, and processed by the horizontal-to-vertical (H/V) spectral ratio technique (**HVSR**). **The resonance frequencies** and their **amplification factor**s were picked from the H/V curves and the **sediment thickness** were derived from the regressive relationship to the resonance frequency. The results show that site response in Beijing area varies significantly: the resonance frequencies span 0.2-10 Hz and the amplification factors are between 2 to 15. The thickness of sedimentary layer varies from a few meters to over eight hundred meters. The inferred sediment thickness profiles reveal some structural features that may associated with possible blind active faults in Beijing are area, such as the northwesterly oriented Sunhe-Nankou Fault that crosses both profiles, and the northeasterly oriented Shunyi-Liangxiang Fault crossing the NW profile. This project is supported by the Institute of Earthquake Science (Project No.0207690229) and Ministry of Science and Technology of China (Project No. 2006DFA21650).

KEYWORDS: **Beijing, Microtremor, HVSR, Resonance frequency, amplification factor, sediment thickness**

1. INTRODUCTION

It has long been recognized that strong ground motion and thereafter earthquake damage is generally larger over soft sediments than on bedrock outcrops. For large cities sited on soft sediments and close to earthquake prone zones, site classification and microzonation for seismic hazards reduction are critical tasks for seismologists and earthquake engineers.

Beijing area is located on the Beijing Plain which is a large alluvial fan, and the central Beijing is on a graben-like basin with deep soft sediment that some borehole data show the Quaternary deposits in some places can reach over 800 meters (IGSB, 2002a,b). Based on years' of geological investigation(Xu et al, 2002), current geological data show that quite a few numbers of blind faults may have developed in the NE direction, including the Qinghe Fault, the Baobaoshan Fault, the Huangzhuang-Gaoliying Fault, the Shunyi-Liangshang Fault, and the the Nanyuan-Tongxian Fault. In the NW direction, such as the Nankou-Sunhe Fault, the Jiuxianqiao Fault, and the Yongdinghe Fault (Figure 1). The fault system controlled the Cenozoic weathering and deposition procession on the geological time and made the basin deposition pattern significantly different. In early Tertiary time, Beijing Plain showed sandwich mode tectonic activities controlled by the NE-oriented structures: the Beijing Depression was clipped by the uplift area in the northwest and the Daxing Uplift in the southeast. However, since late Tertiary, especially in Quaternary time, the sedimentary structure pattern was mainly controlled by the NW-oriented active faults and changed significantly from north to south, where the Shahe

Depression developed in previous NW Beijing Uplift, and the Beijing Depression was evolved into Shunyi Depression and Fengtai Uplift, which joined the Daxing Uplift in southeast (IGSB, 2002a,b 2003a,b; RGSG,1991; Xu et al,2002).

Some segments of the blind faults have been active in history. The 1730 Haidian M~6.5 Earthquake, less than 20km NW of the city center, occurred on the Qinghe fault, which resulted in the maximum intensity IX at the epicenter and VIII in city center. It generated a strongly abnormal intensity distribution. Surrounding Beijing areas are also earthquake prone zones. During the last 500 years (the Ming and Qing Dynasties) there are at least 11 earthquake events with the maximum intensity of VI or greater occurred within the 100km radius from the city center(SSB,1995). The most famous earthquake is the 1679 M~8 Sanhe-Pinggu Earthquake whose epicenter was only about 60 km ENE of the city center, caused Intensity VIII in Beijing city. The much recent 1976 M=7.6 Tangshan earthquake, about 150km from Beijing, also severely affected Beijing with Intensity VI in general and with some abnormal areas above VII (Jiang et al, 1979).

The existence of the thick sediments in Beijing area plays a critical role in estimating the surface ground motion. There are many ways to construct a sedimentary map, such as borehole measurement and active seismic exploration. Both of them are expensive and inconvenient to implement in urban areas. While as an economical and convenient tool microtremor surveys using the horizontal to vertical (H/V) spectral ratio technique, which was first proposed by Nogoshi and Igarashi(1971) and widely spread by Nakamura(1989), have been widely accepted to investigate sedimentary structure (Bard et al, 2004). From H/V curve we can obtain site response parameters (resonance frequency and amplification factor) (Bonnefoy-Claudet et al, 2006a), or infer the sediment depth (Parolai et al, 2002; Delgado et al, 2000). It has also been used to invert the velocity structure (Arai et al, 2004). H/V experiments (Lermo et al, 1996; Fäh, 1997) and simulation (Bonnefoy-Claudet, 2006b) show that the H/V peak frequency can be a good estimate of fundamental resonance frequency regardless of the noise origin; but the amplification factor might be affected by the noise source type. For the purpose of constructing high-resolution map of sediment thickness and site response parameter in Beijing we have conducted several microtremor observations around Beijing area (Chen et al, 2008). One of the observations is the dense linear array measurements along two roughly orthogonal profiles in the NW and NE directions centered at the Forbidden City at the city center. In this paper, we focus our discussion on using the H/V technique to extract geological information from the two profiles.

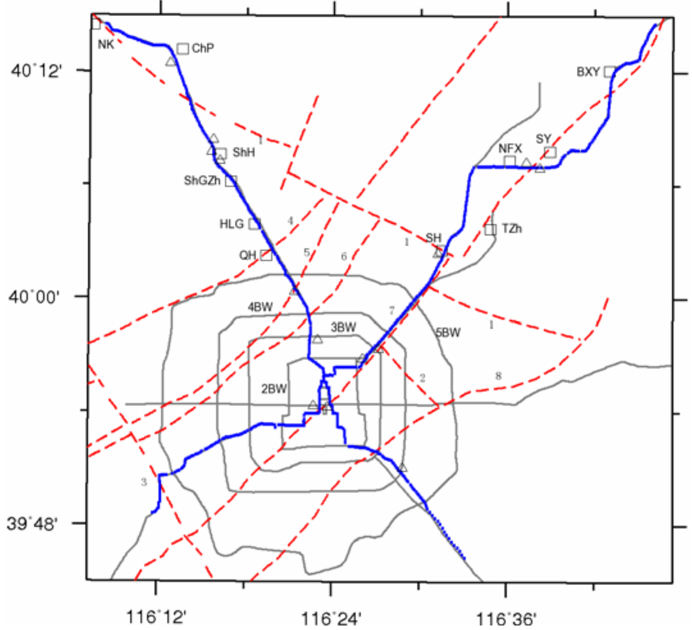

Figure 1 Microtremor measurement sites map. The continuous blue dots are the microtremor observation sites. The triangles are boreholes close to the profiles, from north to south, they are CKB-6, Shui3, Zhen2, 420-37, Qingnong, ZKB045, ZKB127, ZKB193 along the NW profile; Shun4-bu, Repu-1, Shun2, ZKB056, ZKB072,

ZKB123 along the NE profile. The squares are towns along the profiles, where NK: Noukou, ChP: Changping, ShH: Shahe, ShGZh: Shigezhuang, HLG: Huilongguan, QH:Qinghe, BXY: Beixiaoying, SY: Shunyi, NFX: Nanfaxing, Tzh: Tianzhu, SH: Sunhe. Other symbols are the major roadway: 5BW: the 5th Beltway, 4BW: the 4th Beltway, 3BW: the 3rd Beltway, 2BW: the 2nd Beltway. The red broken lines are blind faults; they are: 1: Nankou-Sunhe Fault, 2: Jiuxianqiao Fault, 3: Yongdinghe Fault, 4: Qinghe Fault, 5: Babaoshan Fault, 6: Huangzhuang-Gaoliying Fault, 7: Liangxiang-Shunyi Fault, and 8: Nanyuan-Tongxian Fault

2. DATA ACQUISITION AND PROCESSING

Microtremor data were acquired along two roughly orthogonal profiles in the NW and NE directions centered at the Forbidden City along main highways and roads as shown in Figure 1. The equipment used were 30 Guralp 40T-1 three-component short-period seismometers and 30 Reftek 130B recorders with internal GPS satellite receiver for positioning and time keeping. The sampling rate was 50 Hz throughout the entire field observation campaign.

There were a total of 378 numbered sites in the NE profile, and 322 sites in the NW profile. The spacing between two adjacent sites was 200 meters, positioned with the accuracy of the single-frequency hand-held GPS receivers. Thus, the total length is 76 km for the NE profile and 64 km for the NW profile. All sites in one profile were numbered sequentially from north to south with the header indicating the NW or NE profile. For the NW profile, no data were collected for the odd number sites from NW294 to NW322. For the majority of all the sites, in one measurement epoch, microtremor data were acquired simultaneously using all of the 30 instruments for least one hour. Then the instruments were rolled over forward along the profile to start a new epoch, with the last site of the previous epoch as the first site in the new epoch. To ensure data quality, the observations for most sites within the Fourth Beltway of Beijing (i.e., NW163－NW278 and NE204－NE320) were carried out in night time while other sites in daytime. Though the 2 profiles are designed along major highways and roads and all sites were selected to be as far from the traffic flow as possible to avoid local transient disturbance. As one can image, the locally concurrence of high-amplitude and short duration disturbances are unavoidable in the busy urban area like Beijing. As described below, through data processing the short duration transient noises are excluded in further analysis. The field work was carried out with 5 field vehicles and 20-32 people, which varied from day to day and was completed within 7 days.

In data processing, the three-component microtremor velocity records were DC removed and de-trended first. Then the data were divided into 50-sec long time windows with 10% time overlap. For each time window, a 5% cosine taper was applied and the Fourier spectrum was obtained with 200 frequency intervals from 0.2-15Hz. Then the H/V spectral ratio was derived from the ratio of the root mean squared spectra of the NS and EW components to the vertical spectrum. All spectra were smoothed using the Knonno and Ohmachi (1997) smoothing algorithm (with parameter b =50). The averaged H/V curves for all time windows are presented as the final H/V curve for a given site. For sites in the inner city (NW150－NW260, NE225－NW378) where microtremor data were severely affected by the near-site transient noise we used the anti-STA/LTA (Short Time Average(STA) to Long Time Average(LTA) ratio) algorithm to select relative stationary 25-sec long time window, where STA length was set to be 0.5s, LTA length to be 25s and the STA/LTA ratio range to be 0.2-3.5. For this case the H/V calculation was conducted from 0.4-15Hz instead of 0.2-15Hz as used in the good data sets.

The H/V curves showed complicated pattern. According to our observations there are possibly four types of H/V curve shapes as showed in Figure 2. Type I (Figure 2a) has a clear resonance frequency peak can be recognized automatic by the program. Type II (Figure 2b) shape has two clear peaks with one peak is very sharp and high amplitude. These sharp peaks at 1.5 Hz are continuously seen in the southeast part of the NW profile and keep at the constant frequency of 1.5 Hz. We concluded that this sharp peak is caused by some kind of industrial noise in this area with the majority of energy radiating in the horizontal direction so that the other peak is the true H/V resonance frequency. Type III (Figure 2c) has wide high amplitude in a broad low frequency range. This phenomenon may be caused by weather conditions such as wind interacting with sensors and wires (Mucciarelli et al, 2005). Type VI (Figure 2d) has multi-peaks, which may be due to several impedance layers such as refilled soil in urban construction.

Obviously, picking up the H/V resonance frequency from a single H/V curve is not trivial. To better understands and picks the reasonable resonance frequency, we normalized H/V curve for each sites with its maximum amplitude then plotted those normalized curves side by side to image in site number order. Pickings were done automatic and then adjusted by hand according nearby peak change tendency. Along the 2 profiles there was not enough borehole data for us to fit a resonance frequency(f_r) - sediment thickness (h) relationship, but we found the relationship in Cologne area (Germany) (Parolai, 2002) shown in Eqn. 1 fits our data reasonably well.

$$h = 108\, f_r^{\,-1.551} \tag{1}$$

We have used this relationship to convert the picked resonance frequencies into sediment thickness along the 2 profiles. The geological implications of the sediment thickness are discussed below.

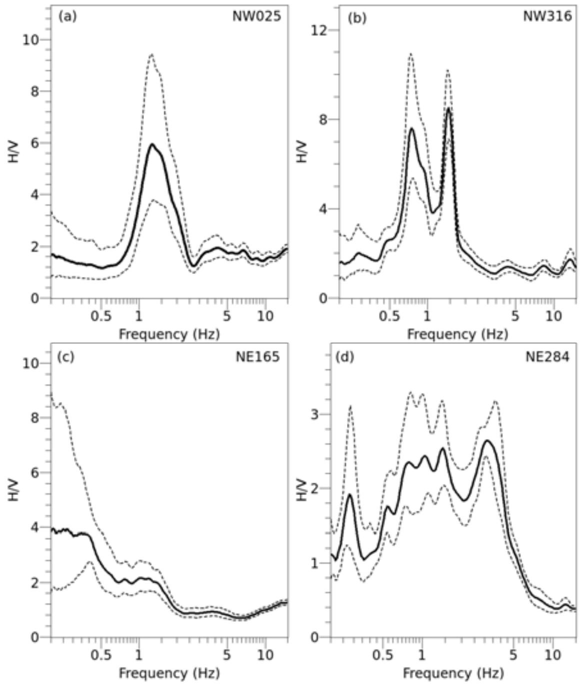

Figure 2 Patterns of H/V curves. The solid lines are H/V curves, the dotted lines are their corresponding standard deviations.

3. RESULTS

3.1 Results from the NW Profile

Figure 3 shows the normalized H/V curves as color images (Figures 3a and 3b), the resonance frequencies and their amplification factors (Figure 3c), the surface elevation along the NW profile (Figure 3d), and the inferred sediment depth (Figure 3e) for the NW profile. The normalized H/V images in Figures 3a and 3b clearly show continuous and traceable peak frequencies in most sites. The differences between Figure 3a and 3b are anti STA/LTA algorithm was used to select time window in order to reduce transient noise's affection, and H/V normalization only considered frequency band from 0.4-15Hz for sites NW150-NW260 where transient and near-site noise may be strong. We can see that the H/V image has only a little improvement in Figure 3b. From site NW200-NW322, we can find that the industrial noise exists continuously with a sharp peak at 1.5Hz. For sites NW054-NW084, besides the resonance frequency lower than 0.5Hz, there is another peak frequency at about 1-2Hz. The higher frequency peaks are not the higher modes of the fundamental resonance frequency, but maybe resulted from the existence of another high impedance interface at shallow depth of the sedimentary layer.

As shown in Figure 3c, the resonance frequencies vary between 0.2-10Hz, while their corresponding amplification factors vary between 2-15 and can change relative rapidly from site to site. The sediment depth profile that inferred from the resonance frequencies using Eqn. 1 and referenced from the surface elevation is shown in Figure 3e. They show strong correlation with surface elevation change along the profile (Figure 3d), such as the syncline near NW025, the abruptly depth drop near NW050, and the slowly deepening after NW255. Based on the elevation and sediment depth drop near Changping (site NW050), we are relatively confident for inferring that the Nankou-Sunhe Fault crosses the profile around this site. From Shahe (site NW082) to the 4th Beltway north (site NW176), the sediment depth gradually becomes shallower, and show apparently a series of thrust structures. Some possible thrust faults may exist here as discussed by Hua et al (2005). The Qinghe Fault and the Babaoshan Fault (Faults 4 and 5 in Figure 1), due to their possible locations may be associated with site NW131 and NW155, respectively, where both have apparent resonance frequency changes. Sites NW176-NW195 have distinct frequency drop which may be related to Huangzhuang-Gaoliying Fault (Fault 6 in Figure 1) at northern part while at the southern part may be related to another possible fault, Chegongzhuang-Deshenmen fault, as mentioned in reference RGSG(1991). The depressed segment from site NW218 to NW256 may be a graben formed by the Liangxiang-Shunyi Fault (Fault 7 in Figure 1) as the north edge and the Nanyuan-Tongxian fault (Fault 8 in Figure 1) as the south edge. The sediment depths for sites south of NW257 are gradually increased, mimicking the same downward trend of the surface elevation.

As a reference, the vertical bars superimposed on the depth profile in Figure 3e are basement depths from boreholes within 600 meters from the sites. Most of them are comparable to inferred sediment depth. This fact implies that Eqn. 1 can be reasonably applied in Beijing area.

3.2 Results from the NE Profile

Figure 4 shows the normalized H/V curve images (a and b), the resonance frequencies and their corresponding amplification factors (c), the surface elevation along the profile (d), and the inferred sediment depth (e) for the NE profile. In Figure 4b sites NE225-NE378 were used the anti-STA/LTA algorithm to select time window, we can also see only a little improvements in the H/V image. Similar to NW profile, most sites have continuous and traceable peak frequencies except for the sites from NE160 to NE220, where many of their H/V curves dipped to low frequency and showed no peak frequencies. Since those sites were set by different groups of operators in 2 observation epochs and the horizontal component at all sites have seen strong low-frequency energy, we suspect that during the time of observation there had been strong wind affected those seismometers and caused this phenomena. At sites NE54-NE220 and NE282-NE378, other intermittent peak frequency interfaces also appear at higher frequency than resonance frequency.

As shown in Figure 4c, the highest resonance frequency is about 8Hz at NE20 where we can also see bedrock outcrop out nearby. The lowest resonance frequencies are found between sites NE50 to NE172, which corresponding to the Shunyi Depression while the inferred sediment depth for these sites have ranged from 400 to 800 meters. The sediment depth also has good correlation with the surface elevation, except for the sites beyond NE282. The NE profile crosses the Liangxian-Shunyi Fault twice, near the site of NE50 and NE100 where both have distinct depth drops and surface elevation changes. The Nankou-Sunhe Fault may locate nearby NE172 and we can see that at this part of the fault the dropping wall is on the north side while at the NW profile the dropping wall is on the south. Though after NE225 the H/V curves have poor qualities to clearly pick the peak frequencies, we can still guess the Jiuxianqiao Fault may be associated with sites NE217–NE232, and the Yongdinghe Fault may be associated with site NE355.

4.CONCLUSIONS

Microtremor measurements along two profiles in the NW and NE direction processed with the H/V spectral ratio technique have given encouraging results in Beijing about site response parameters, sediment depth. The resonance frequencies span from 0.2Hz to 10Hz with high amplification factors greater than 2. The sediment depth undulates significantly from several meters to over eight hundred meters. Some blind faults such as Nankou-Sunhe Fault and Shunyi-Liangxiang Fault can be revealed by interrupting sedimentary depth variations.

Some factors for example weather and near-site transient noise will severely affect the H/V results. The weather conditions such as wind caused some sites in the NE profile useless. In urban area, most sites within the 4th beltway in the two profiles have peak frequency with more ambiguity which may due mainly to the near-site transient noise. As a fast and economical exploration tool for seismic hazard study to be continuously in the future site selection and weather awareness are two key issues to ensure high quality data acquisition.

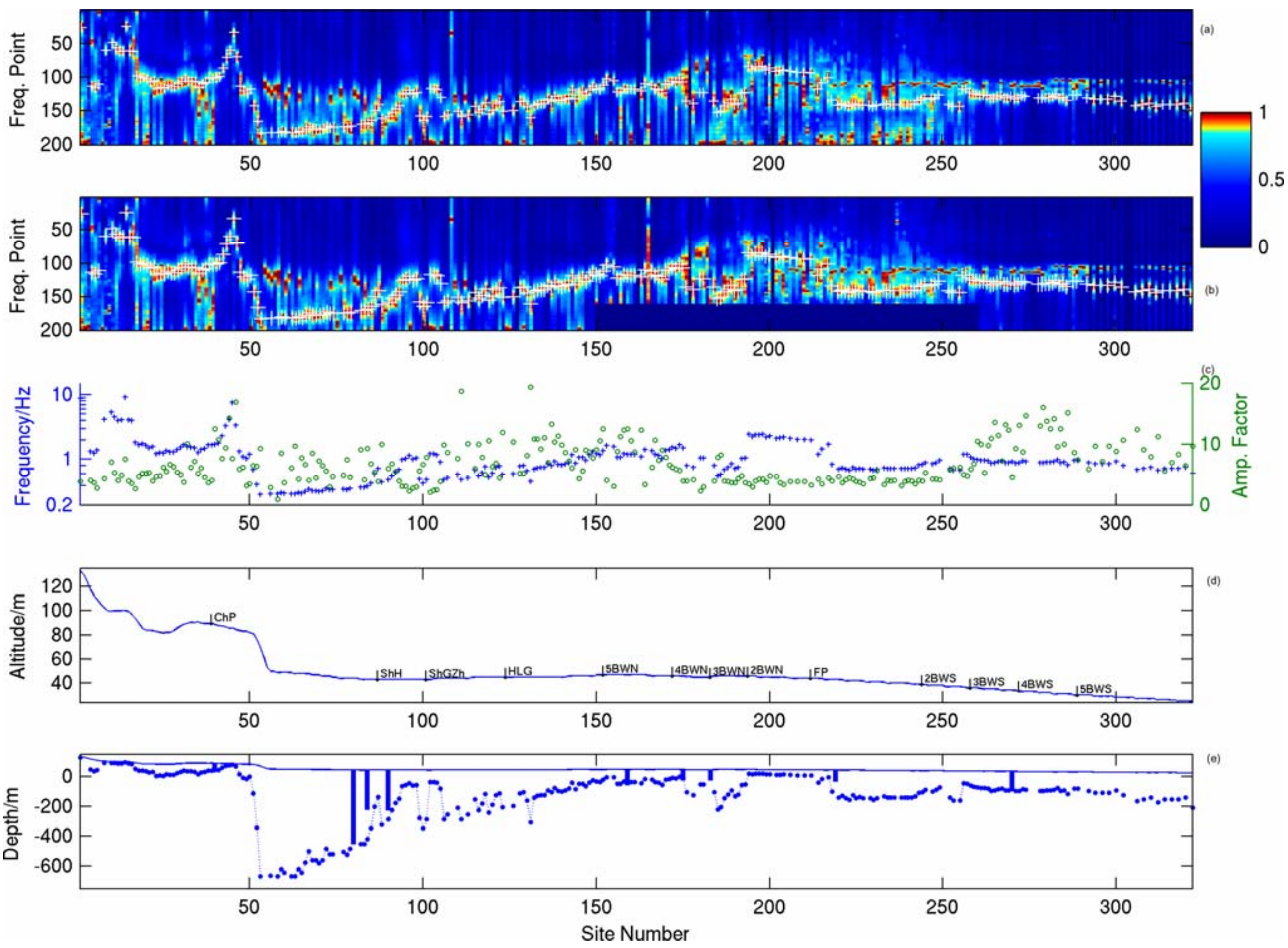

Figure 3 The H/V results for the NW profile. (a) Normalized H/V curves image. Y-axis is frequency point number corresponding to 15-0.2Hz from up to down. (b) Normalized H/V curves image. Where for sites NW150-NW260 time windows were selected with 25s time length and anti STA/LTA algorithm and only 0.4-15Hz bands were considered in H/V normalization. (c) Picked resonance frequencies (+) and their corresponding amplification factor (circle). (d) The altitude of the profile, subtracted from 1:250000 DEM data. (3) Sediment depth inferred from resonance frequency. Where solid line is altitude; bars are borehole around the profile, they are CKB-5, Shui3, Zhen2, 420-37, Qingnong, ZKB045, ZKB127 and ZKB193 from left to right.

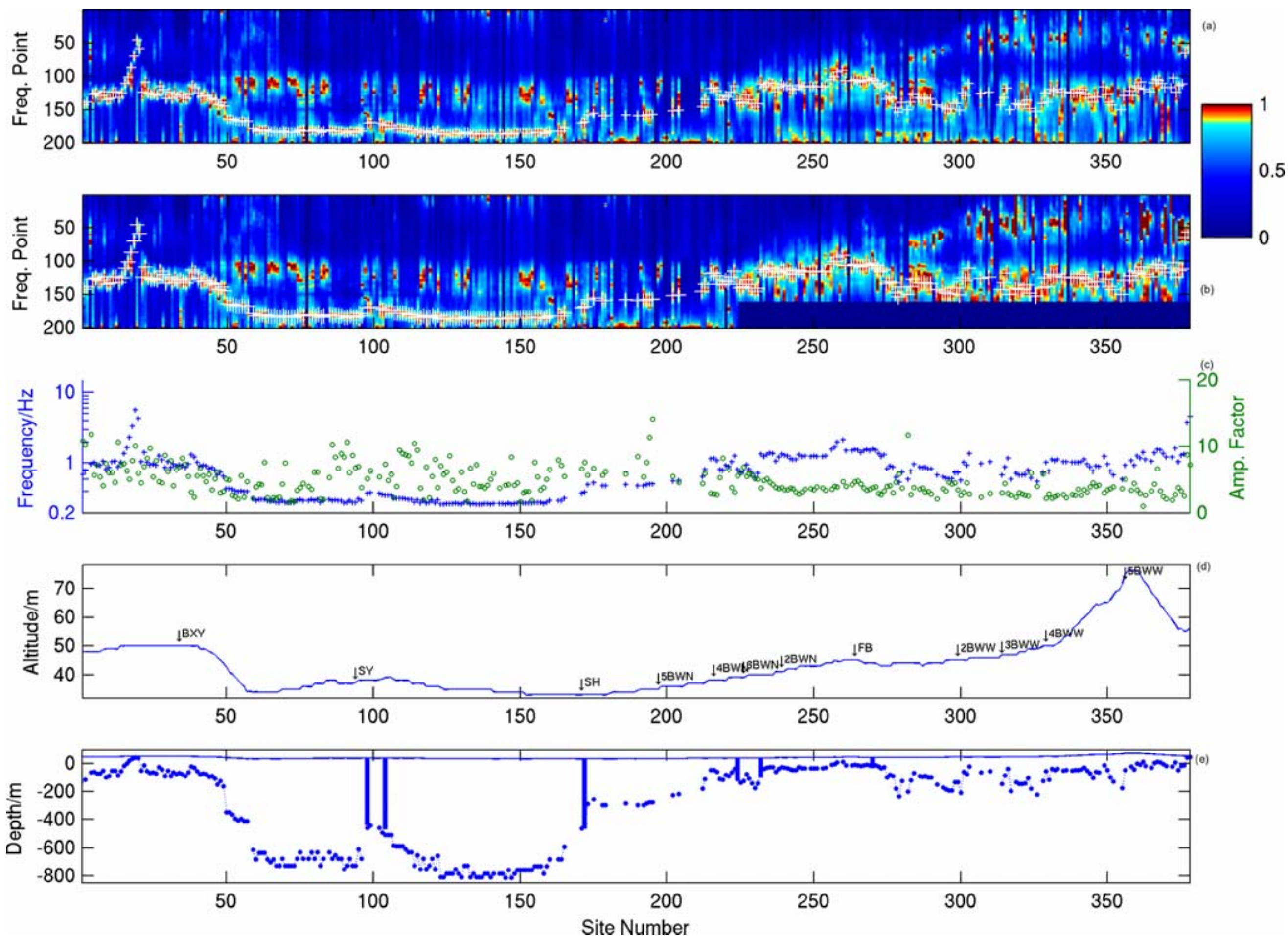

Figure 4 H/V results for NE profile. (a) Normalized H/V curves image. Y-axis is frequency point number corresponding to 15-0.2Hz from up to down. (b) Normalized H/V curves image. Where for sites NE225-NE378 time windows were selected with 25s time length and anti STA/LTA algorithm and only 0.5-15Hz bands were considered in H/V normalization. (c) Picked resonance frequencies (+) and their corresponding amplification factors (circle).(d) The altitude of the profile, subtracted from 1:250000 DEM data. (3) Sediment depth converted from resonance frequency. Where solid line is altitude, bars are borehole around the profile, are Shun4bu, Repu-1, Shun2, ZKB056, ZKB072, ZKB123 from left to right.

REFERENCES

Arai, H., Tokimatsu, K. (2004). S-wave velocity profiling by inversion of microtremor H/V spectrum. Bull Seism Soc Am, 94:53~63

Bard, P. Y. and Sesame Participants. (2004). The SESAME project: an overview and main results. Proceedings of the 13th World Conference on Earthquake Engineering, Vancouver, Paper 2207.

Bonnefoy-Claudet, S., Cornou, C., Bard, P. Y., Cotton, F., Moczo, P., Kristek, J. and Fäh, D. (2006). H/V ratio: a tool for site effects evaluation: results from 1D noise simulations, Geophys J, 167, 827–837.

Bonnefoy-Claudet, S., Cotton, F., Bard, P. Y., Cornou, C., Ohrnberger, M. and Wathelet, M. (2006).Robustness of the H/V ratio peak frequency to estimate 1D resonance frequency. Third International Symposium on the Effects of Surface Geology on Seismic Motion, Grenoble, France, 2006,Paper 85 1

Chen, Q.-F., Liu, L., Wang, W. and Rohrbach, E. (2008) Site effects on earthquake ground motion based on microtremor measurements for metropolitan Beijing, Chinese Science Bulletin, in press. (in Chinese)

Delgado, J., Lopez, C. C., Estevez, A. C. and et al.(2000). Microtremors as a geophysical exploration tool: applications and limitations. Pure Appl. Geophys., 157, 1445–1462.

Fäh, D. (1997). Microzonation of the city of Basel. J. Seismology, 1(1),,87-102.

Hua, J. R., Hou, G. T. and Liu, X. D.(2005).Study of the Active Faults Generating the Earthquake of ML 61/2 in the West of Beijing in 1730. Acta Scientiarum Naturalium, 41(4):530-535. (in Chinese)

Institute of geological survey of Beijing (IGSB). (2002a).Report of regional geological survey for Yanqing (J50 C 004002, Map scale 1:2500000), P. R. China. (in Chinese).

Institute of geological survey of Beijing (IGSB). (2002b).Report of regional geological survey for Beijing (J50 C 001002, Map scale 1:2500000), P. R. China. (in Chinese).

Institute of geological survey of Beijing (IGSB). (2003a).Report of regional geological survey for Shunyi (K50E 024011, Map scale 1:50000), P. R. China. (in Chinese).

Institute of geological survey of Beijing (IGSB).(2003b).Report of regional geological survey for Shahe (K50E 024010, Map scale 1:50000), P. R. China. (in Chinese).

Jiang, P., Wang, Q. M., Xu, F. and Cui, J. L.(1979). Discussions on the reasons of several abnormal destroy regions after Tangshan Earthquake. Seimic Geology, 1979, 1, 90-98. (in Chinese).

Konno, K. and Ohmachi, T. (1997) Ground-motion characteristics estimated from spectral ratio between horizontal and vertical components of microtremor. Bull Seism Soc Am, 88: 228-241.

Lermo, J. and Chavez-Garcia, F. J.(1994). Site effect evaluation at Mexico city: dominant period and relative amplification from strong motion and microtremor records. Soil Dyn and Earthq Eng, 13, 413-423

Mucciarelli, M., Gallipoli, M. R., Giacomo, D. D., Nota, F. D. and Nino, E. The influence of wind on measurements of seismic noise. Geophys J Int, 161, 303–308.

Nakamura, Y. (1989). A method for dynamic characteristics estimation of subsurface using microtremor on the ground surface. Q Rep Railway Tech Res. Inst , 30, 25–33.

Nogoshi, M. and Igarashi, T.(1971). On the amplitude characteristics of microtremor (part 2). J Seismol Soc Japan, 24, 26-40.

Parolai S, Bormann P and Milkereit C.(2002). New relationships between Vs, thickness of sediments, and resonance frequency calculated by the H/V ratio of seismic noise for the Cologne area (Germany). Bull Seism Soc Am, 92：2521–2527.

Regional geological survey group of Beijing Geological Research and Testing Center (RGSG). (1991). Report of regional geological survey for Beijing (J-50-5-B, Map scale 1:50000), P. R. China. (in Chinese).

State Seismological Bureau (SSB). (1995). Atlas Catalogue of Historical Strong Earthquakes in China (23 B.C. to 1911 A.D.). Seismological Press, 44-471. (in Chinese).

Xu, X. W., Wu, W. M., Zhang, X. K. (2002). Newly tectonic structure development and earthquake at Chinese capital region. Science Press, Beijing. (in Chinese).